Chapter 2
3D Diffractive Lenses to Overcome the 3D Abby Diffraction Limit

Abstract Radiation cannot be focused on anything smaller than its half of wavelength—or so says more than a century of physics wisdom. In the first part of this chapter the results of the focal fields of a phase correcting Fresnel lens examination are described for several small values of *F*/, with $F \leq 2\lambda$ which allows for overcoming Abbe barrier. It was also shown that the minimum diameter of the focal spot near the central circumferential step of binary diffractive axicon was equal to FWHM = 0.38λ. In the second part of this chapter the innovative radiating structures as a conical FZP lens are proposed for subwavelength focusing. It has been shown that in contrast to the flat diffractive optics the curvilinear 3D diffractive conical optics allows for overcoming 3D Abbe barrier with focal distance F more than F > 2λ.

Keywords Abbe barrier · Diffractive lens · Superresolution · Axicon · 3D optics · Near field

Introduction

Many attempts have made to improve the resolving power of optical imaging systems since Ernst Abbe discovered that the resolution of an imaging system is limited by diffraction. Diffraction, as a general wave phenomenon which occurs whenever a traveling wave front encounters and propagates past an obstruction, was first referenced in the work of Leonardo da Vinci in the 1400s [1] and has being accurately described since the Jesuit astronomer, mathematician and physicist Francesco Grimaldi in the 1600s [1] and by the Scottish mathematician J. Gregory in 1673,[1] who studied the dispersion of white light into a spectrum using a feather. Wave diffraction is a phenomenon that manifests itself as a departure from the laws of geometrical optics under wave propagation.

The erratum to this chapter is available at DOI 10.1007/978-3-319-24253-8_7

[1]Rigaud [2].

I. Minin and O. Minin, *Diffractive Optics and Nanophotonics*,
SpringerBriefs in Physics, DOI 10.1007/978-3-319-24253-8_2

The possibility to obtain subwavelength resolution utilizes a highly focused near-field spot of a hemispherical lens with a high refractive index in millimeter wave was demonstrated at [3]. In [4] authors demonstrate that in the near-field of a hemispherical sapphire lens a resolution of $\sim 0.3\lambda$ can be obtained for millimeter-wave frequencies. It was mentioned that the first Teflon™ lens with a focal ratio F/D ~ 1, focuses the beam to a diffraction-limited spot. Without a hemispheric sapphire lens the spot size would be approximately one wavelength.

For optical and quasi-optical applications, lenses are typically designed with values for F/D much larger than one, due to the physically small values for the wavelength. It could be noted due to smaller wavelength, mm-wave lens antennas and lenses rely heavily on the quasioptical principles.[2] These lenses thus have spatial resolutions much greater than a wavelength. At microwave, millimetre-wave and THz frequencies, since the wavelengths are much longer, as well as in microoptics and nanooptics, it is feasible to design lenses with values of $F/D < 0.5$. For these values, the equation $\Delta = 0.61\lambda/\mathrm{NA}$ is no longer an accurate estimate of the resolution. It was not clear what spatial resolution can be obtained for such designs. Moreover, for small values of F, the focal spot is in the reactive near field of the lens, and the effects of these reactive field components cannot be neglected, as is the case for larger values of F [5].

A new study now shows that it is possible to focus radiation less than half of wavelength, if radiation is focused extremely close to a special kind of "superlens". Diffractive optical elements (DOE)—flat analog of a lens—zone plates (ZP[3]), was a simplest example of DOE. Next, transparent phase gratings and zone plates with a diffractive microrelief were invented, in which the transition from dark to light regions corresponded to a stepwise jump by a quality of the order of wavelength λ, ensuring a wave phase incursion for π.

The values of $F \leq \lambda$ are of interest because the subwavelength resolution may be observed. For example, according to Heisenberg's uncertainty principle, it is impossible to determine the product of the uncertainties of the position of a particle and its momentum to better than h (actually h/2π): $(\Delta x)(\Delta p_x) > h$ and in scattering of photons in the maximum range of angles, $\Delta x \geq \lambda/2$. However, if we restrict one of the components of the wave vector, it will vary the other components of the wave vector. For example, let $k_y = 0$, $k_z = -i\gamma$, where γ—a positive real number. Than if $\gamma \rightarrow 0$, the range of permissible values of k_x grows indefinitely, and Δx can be arbitrarily small. Imaginary values of k_z correspond to damped waves.

[2]In "quasi-optical systems" the diffraction effects are inevitably important because of although radiation is typically propagated and analyzed as free-space beams, unlike traditional optics, in MMW and THz beams may be only a few wavelengths in diameter. See [5].

[3]The classical Fresnel zone plate, consisting of a plane array of alternately opaque and transparent concentric circular rings, acts upon a normally incident plane wave, transforming it into a converging wave and concentrating the radiation in a small region about a point on the axis. The zone plate is an image forming device, but the mechanism involved for this simple screen is not refraction at the boundary between different dielectric media, but diffraction at the series of annular apertures and subsequent interference of the diffracted radiation.

Consequently, the implementation of subwavelength resolution antenna probe must be within the evanescent field near the surface of the sample, that is certainly at $Z < \lambda$ [6].

It should be noted that *diffractive focusing elements* are crucial components of major range communications and instruments nano systems. Their design and manufacturing would be much faster and cheaper if one could avoid costly prototyping and measurements. To minimize design delays as well as to propose innovative radiating structures, it is necessary *to develop a scale model.* So investigations in millimeter wave/THz taking into account the scale effect may be transfer directly to optical and nanooptical bands.

Flat Diffractive Lens with Superresolution

The binary phase-correcting Fresnel lenses [7, 8] were consist of a set of annular dielectric rings whose radii were determined using the traditional Fresnel zoning rule for flat surfaces with the geometric optics approximation:

$$r_i = \sqrt{Fi\lambda + \left(\frac{i\lambda}{2}\right)^2}, \quad i = 1, 2, \ldots N \tag{2.1}$$

where F is the focal length of the lens, λ is the wavelength, r_i is the radius of the ith Fresnel zone, and N is the total number of zones in the lens of diameter D. (It should be noted that the optimisation of the Fresnel zone radii [9] for improved focusing was not the aim of this study). The thickness (t) of the rings is calculated based on the requirement of achieving a 180° path difference between the waves travelling through the dielectric rings and those travelling through air:

$$t = \lambda/[2(\sqrt{\varepsilon_r} - 1)] \tag{2.2}$$

where ε_r is the dielectric constant of the rings. Three lenses were designed using a dielectric constant of $\varepsilon_r = 4$, which from (2.2) result in a ring thickness of $t = \lambda/2$. The focal lengths for the lenses were chosen to be 2λ, 1λ, and 0.5λ. The diameters for the three lenses are somewhat different since an integer number of zones was used for each case; the values were chosen as close to $D/\lambda = 10$ as possible.

The focusing behaviour for the case of an incident plane wave, polarized in the y-direction, was investigated using finite difference time domain (FDTD) analysis[4] [9–14].

The simulated focal fields in the y-z plane (at $x = 0$) are shown in Fig. 2.1, where the focal spots are seen to the right of the lenses. For all three lenses, the maximum

[4]FDTD simulation of flat FZP was developed in cooperation with N. Gagnon and A. Petosa from Communications Research Centre, Canada.

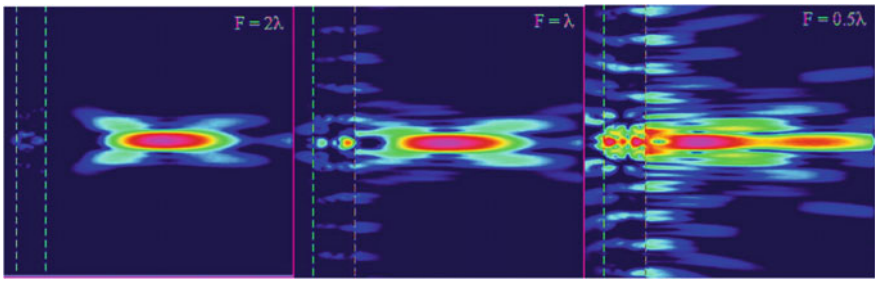

Fig. 2.1 Normalized power density in the y-z plane for the three Fresnel lens designs

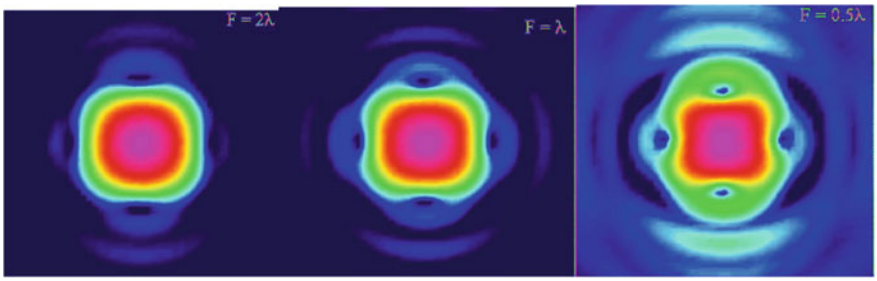

Fig. 2.2 Normalized power density at the distance of maximum intensity (focal spot)

intensity occurs close to the designed focal length. This can be better observed in Fig. 2.2, which plots the power density (normalized to the peak value) along the focal axis ($x = y = 0$). The results of experimental verifications [6] confirm all FDTD simulation results. Since the spot beams were not perfectly axially symmetrical, the spatial resolutions in both the *x*- and *y*-planes are listed (both FWHM and determinated by the 1st minimum). Except for one case ($F = 2\lambda$), the spatial resolutions are all less than 0.5λ, which is significantly finer than the spatial resolution achieved from lenses with large values of *F/D*.

This investigation on the focusing properties of phase correcting Fresnel lenses with values of $F/D < 0.2$ and with $F \leq 2\lambda$ has shown that a spatial resolution of less than 0.5λ is achievable. Also from the Fig. 2.2 it is followed that except for one case ($F = 2\lambda$), the axial resolutions are all less than 2.0λ, which is significantly finer than the axial resolution achieved from lenses with large values of *F/D*. So the "Abbe barrier" was thus completely broken by such diffractive lenses with unique 3D super resolution [6, 14, 15]. As the *F/D* values decrease, so does the spot beam size and thus a finer resolution is achieved. Although the spot beam decreases with decreasing *F/D*, the total amount of focusing power also decreases (Fig. 2.3). There is thus a trade off between refined resolution and focusing power, and the selection of the *F/D* will thus depend on the intended application.

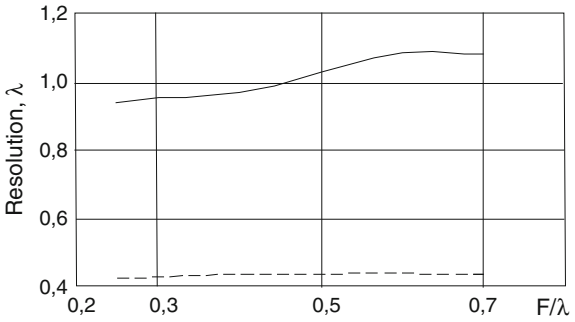

Fig. 2.3 Average resolving power versus F/λ for x-axis (*solid line*) and y-axis (*dashed line*)

The reason for the slight axial asymmetry in the intensity patterns arises from the anti-symmetrical component of the electric field in the z-direction (direction of the incident wave). This component is significant for small values of *F/D*, since the focal spot is in the reactive near-field of the lens, and it causes the slight asymmetry in the intensity patterns (Fig. 2.3). As the values for *F/D* increase, the amplitude of this component quickly decreases and thus does not contribute significantly to the intensity, resulting in a symmetric pattern. In this near field ($F \sim \lambda$) we may talk about evanescent waves, which are waves that are non-homogenous, non-propagating, and exponentially decaying away from the object's surface. They have a complex wave vector perpendicular to the surface and thus allow high wave vectors in the other two directions (i.e. in the plane of the sample). Large k-vectors correspond to small dimensions in direct space, and small directions imply high resolution. Due to the presence of this significant amount of Z polarised light, in the form of a dumbbell along the X axis, the resultant focal intensity distribution is not circularly symmetric [16].

Because of the focal spot in the high NA cases is no longer an Airy pattern and have no circular symmetry it is needed to offer a new criterion of 3D resolution in this case.

Thus in the papers [14, 15] at the first time it were demonstrated that in the near field of single diffractive lens without of the immersion medium a resolution of 0.3–0.4λ can be obtained and the focal spot is slight asymmetry and is no longer an Airy pattern. Moreover, compared to well-known scanning microscopy, this diffractive lens allows simultaneous imaging of a finite area close to the focus.

Later in [17, 18] these results were confirmed in optical wavebands.[5] For example, in [17] numerically and experimentally the focusing of linearly polarized light using the Fresnel ZP with a focal distance of 0.79λ was studied. An elliptical focus spot was experimentally observed with the least diameter by the intensity decay halftime FWHM = 0.63λ.

[5]Dr. Rakesh G. Mote has not come across papers [14, 15]. R.G. Mote, private communication, 2015.

Five years later researches in the optical range [19] also were fully confirmed the results of earlier studies in the millimeter range [14, 15]. In [20] also it was shown that the ability of overcoming the diffraction limit using a zone plate with radius R = 20λ, F = λ and R-TEM 01 mode with radius ω = 10λ is possible. In [21] it was show that the near-field subwavelength focusing can be obtained: with the parameters of the FZP as D = 0.6 μm and F = 0.5 μm (F = 0.79λ), the FWHM was in the range of 0.371λ–0.374λ. The symmetry of focal spot was not investigated.

Thus a high linear resolution may be achieved by using a Fresnel (or Soret) zone plate with NA greater than almost one. The focusing element (lens) can employ also a modified zone plate with an opaque central part which makes up not less than about 50 % of the entire surface area of the plate, in which the radii of Fresnel zones are calculated by taking into account the reference phase concept [7, 22, 23]. But in this case the apodization effects are large.

The principle of the combined zone plate with high NA based on the arbitrary linear phase shift of the radiation passed through one section relative to the radiation passing through the other section also allow to increase the resolution in focal spot. Due to interference effects the sum of the first diffraction orders of the radiation passed through the various sections, the phase shift provides amplification of the longitudinal components of the electromagnetic radiation provided perpendicularity of lines dividing sections of the plane of polarization of the incident radiation. The longitudinal component of the electromagnetic field for FZP with high NA is much stronger and more localized on the optical axis than transverse components of the electromagnetic field. So the introduction of a linear phase jump perpendicular to the direction of linear polarization leads to exclusion in the center of the focal region of the transverse components and the appearance of the longitudinal component of the electromagnetic field. Thus, the prevalence of longitudinal components leads to the reduction of the diameter of the focal spot up to subwavelength size and also decreases the asymmetry of the focal spot due to the attenuation of the transverse component of the electromagnetic field. For the diffractive optical elements (FZP) the introduction of linear phase shift it is possible to realized by means of so-called reference phase concept [7, 22, 23].

The simulation results of photon sieve FZP investigation in millimeter wave had shown [12] that the resolution power of photon sieve FZP is the same as for classical FZP. The reason is on the small number of holes in the FZP aperture. But the first side lobes suppressed conveniently. So the idea of the photon sieve application to millimeter wave optics does not allow increasing the resolution power. But as it known nano-optics deals with optical effects occurring if light interacts with matter that has artificially structured features with sizes comparable to the wavelength.[6] From this point of view, we detailed [12] how the use of simple scale computational experiments in millimeter wave [9] allows obtaining insight into physical systems which are characterized by nanometric objects because of the D/F and D/λ are almost the same.

[6]Novotny [24].

Subwavelength Focusing with Binary Axicon

Demand for improved resolution has stimulated research into developing methods to image beyond the diffraction limit based on different types of optical element including diffractive axicon [7]. As it well known from the Bessel beam theory, the radial distribution of such beam does not depend on the propagation distance z. The effective width of the central peak can be extremely narrow (approximately 3λ/4 far from axicon surface) over large distances.

In millimeter wave/THz if we use a point-like of radiation source in the geometrical optic approximation the radii of zones in the flat axicon surface may be determinates as follows [25]:

$$\sqrt{F^2 + r_k^2} + r_k \sin\gamma = \sqrt{F^2 + a^2} + a\sin\gamma + k\lambda,$$

where k = 1, 2,…, N, r_N = D/2, γ—the angle of rays which crossed the optical axis, a—additional free parameter so-called reference radii [26]—see Fig. 2.4.

So

$r_k = -c\frac{\sin\gamma}{\cos^2\gamma} + \frac{1}{\cos^2\gamma}\sqrt{c^2 - F^2\cos^2\gamma}$, where

$c = \sqrt{F^2 + a^2} + a\sin\gamma + k\lambda$.

The resulting expression shows that in contrast to plane wave illuminating the period of such zones in the diffractive element is not constant, but varies along the radius.

To simplify the problem let's consider axicon with plane wave illumination and with reference radius equal to zero. Binary axicon had a height of step as H = λ/2 (n − 1), the index of refraction n = 1.46. The width of the steps were d = 1.2λ, the period was T = 2d = 2.4λ. The diameter of the axicon was 5 periods D = 12λ. The frequency was equal to 100 GHz. The FDTD simulation showed (Fig. 2.5) that with increasing wavelength λ the focal spot is formed closer to the top of the axicon surface, and its diameter in wavelengths decreases [27, 28]. Also studies have shown that at small distances from the axicon surface (z < 10 wavelength) observed the ellipticity of focal spots (eccentricity of the ellipse about 0.63–0.65), which extended along the linear polarization vector of the incident wave on the axicon.

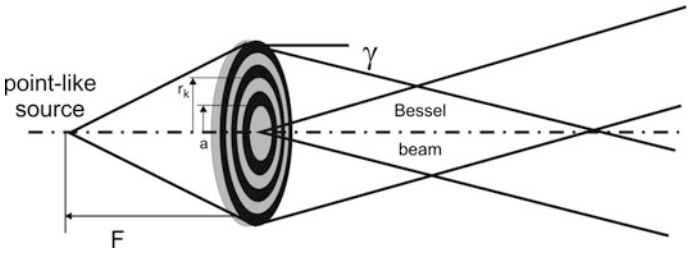

Fig. 2.4 Definition of the binary axicon structure

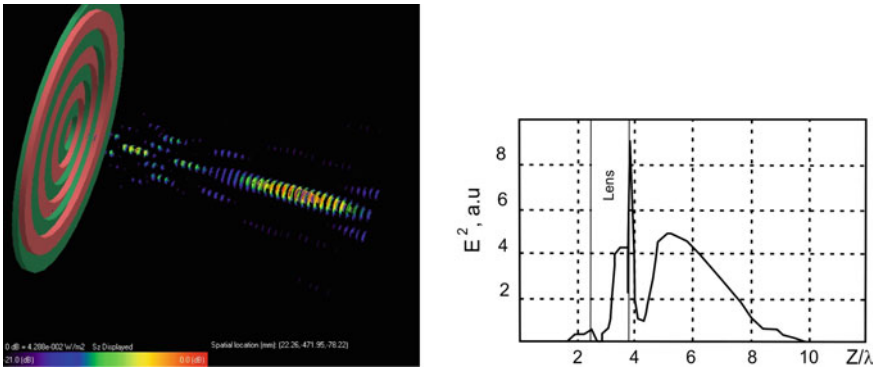

Fig. 2.5 FDTD simulation of axicon focusing (*left*) and field intensity distribution $|E|^2$ along optical axis of optimized binary diffractive axicon (*right*)

The minimum diameter of the focal spot near the central circumferential step was equal to FWHM = 0.38λ and formed at a distance from the axicon surface, about half of wavelength of radiation. Although the present study is at the THz frequency, the principle can be extended to the optical and nanooptical region straightforwardly.

Zoned Metamaterial Lens

A 1.5λ-thick planoconcave zoned lens based on the fishnet metamaterial was investigated experimentally at millimeter wavelengths in [29].The lens was designed to operate at λ = 5.29 mm, where it behaves as an effective negative refractive index medium n = −0.25, with a focal length of F = 9λ. The depth of focus, defined as FWHM along z-axis at the focal length, obtained from experiment was 3.24λ. The sidelobes levels were about 15 %. The symmetry of focal spot was not investigated. To reduce a sidelobes levels the principle of reference phase was successfully apply to the cylindrical fishnet metalenses designed with a $F = 4.5\lambda_0$ and a value of focal length to lateral size ratio (*F/D*) of $F/D_{xz} = 0.214$ and $F/D_{yz} = 0.207$ in the *xz*- and *yz*- planes, respectively (where D_{xz} and D_{yz} are the lateral size of the lens in the *xz*- and *yz* planes, respectively) at [30].

3D Diffractive Conical Lens

Subwavelength resolution beyond the Abbe barrier described above is possible for flat diffractive lens (DOE) only with $F < \lambda$. Below we describe the unique possibilities of 3D subwavelength resolution focusing for 3D diffractive lens with $F > \lambda$.

It is well known [7, 22], that a Fresnel zone plate can be produced conformable to some curvilinear formations. And curvilinear lens can be made on an arbitrary-shaped 3D surface, but the FZP-like lens with a rotational symmetry surface has better radiation characteristics and not only the phase function, but also the 3D surface shape are free parameters that can be used for focusing characteristics optimization, including resolution power both for operating with quasi-monochromatic radiations and femtosecond pulses [31, 32]. The advantages of 3D FZP lens are they have more levels of design freedom and optimization. For example, the conical FZP lens can be easy manufactured at millimeter wave and/or terahertz frequencies as a multilayer assembly of dielectric rings embedded in air space or solid dielectric.

The innovative radiating structures as conical millimeter wave FZP lens and lens antenna at were first proposed by the authors in 1991 (Fig. 2.6), described and studied both theoretically and experimentally in [7, 22, 33]. Like the plane phase-reversal flat FZP lens, the cone-shape zone plate lens transforms in a step-wise manner the incident plane wave into a spherical wave converged in geometrical-optic approximation to the primary focus F [33].

As it was shown theoretically and experimentally the longitudinal resolving power and depth definition (axial resolution Δ_z) can be controlled by choosing the flexure of the diffractive lens surface [7]. The specific behavior of axial resolution of diffractive optical elements on a non-flat surface [7, 22] makes it possible to design systems that possess much higher 3D resolution power and gain than other known classical lenses. Therefore, the main conclusion is that the longitudinal resolving


СОВЕТСКАЯ РОССИЯ ◆ 8 февраля 1991 г. ◆ № 28 (10479) ◆ 2

Антенна близнецов

Братья Игорь и Олег Минкины работают в Институте прикладной физики Сибирского отделения Академии наук СССР. Проблема, которой они занимаются, связана с завтрашним днем нашего спутникового телевидения. Творческая группа, в составе которой работают братья Минкины, подготовила документацию для серийного производства спутниковых антенн из нетрадиционных материалов. На снимке: научные сотрудники Игорь и Олег Минкины.

Фото Б. Евсеньева.

Fig. 2.6 Prototypes of the conical, spherical, parabolic and ogival-shape mm-wave antennas 1991

power of the diffractive optical element can be controlled by choosing the flexure of the diffractive optical element surface and its spatial orientation [7, 8]. Also the latter important effect is due to the reduced FZ lens spherical aberration and to the reduction of the zone shadowing effect in diffractive optical elements on curvilinear surfaces [7, 31]. It could be noted that by selection of diffractive optic surface and its orientation it is possible to minimize the selective types of aberrations [34].

Results of Investigations

Some details about the experimental setup and experimental technique can be found at [7, 35]. First, as an example, we briefly consider a diffractive optical element fabricated on a conical surface which was studied by the authors in 1983 [7, 22]. It was manufactured of a numerically controlled lathe, using optical-grade polystyrene with the following optical constants: diffractive index n = 1.59 and absorption coefficient k $\sim 10^{-3}$. The nominal radiation wavelength was λ_0 = 4.6 mm, lens aperture $D/\lambda_0 = 44$ and the rear segment F = D (lens factor F/D = 1). The maximum flexure of the diffractive lens surface was $<x>/\lambda = 32$. The Fresnel number of lens is 138.

An analysis of the results [36] obtained shows the following:

- half-width (at half-height) of field intensity distribution along the optical axis for a "conical" diffractive optical element, with parameters as shown above, is twice as narrow as that of an equivalent zone plate (when radiation is incident on the side of the apex of the diffractive optics);
- when radiation is incident on the side of the base of the DOE, the width of field intensity distribution along the optical axis is approximately 2.5 times wider than for the equivalent zone plate;
- the shape of this distribution, plotted in relative units, varies very little (by about 3 %) in the range of wavelengths that deviate from the nominal value by less than ±17 %;
- as wavelength decreases in comparison with the nominal value, the intensity of the first side lobe increases; this is the lobe that is located further from the zone plate relative to the distribution maximum. The amount of increase of relative intensity approximately coincides with the amount of wavelength detuning.

Now, consider briefly the conical diffractive lens with small diameter. The parameters of the diffractive lens (Fig. 2.7) both binary and phase correcting was selected as follows: F/D = 1.26, $D/\lambda = 20$ (the dimension of lens diameter was limited by the computer's capabilities), $F/\lambda = 25$, $90 < \alpha < 20$, the lens material was polystyrene (n = 1.59). In the case of binary conical FZP the lens consists of several metal screens of different annular hole normal to optical axis and situated along the conical surface [7, 22]. The results of FDTD simulation of different type of conical phase reversal zone plate with different cone angle are listed below in Fig. 2.8.

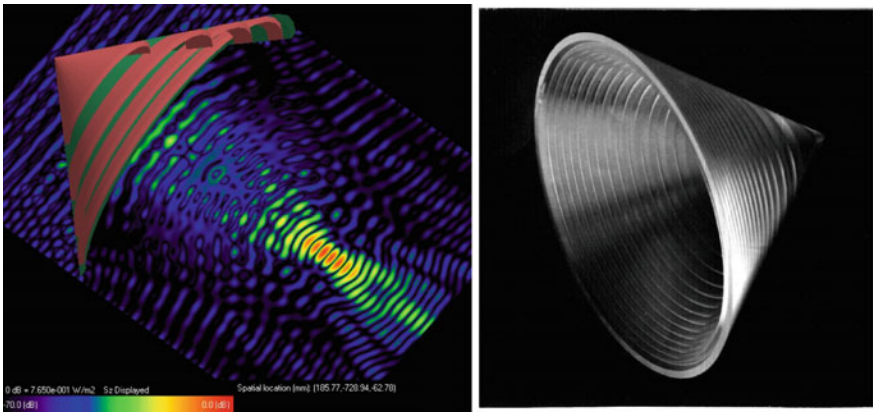

Fig. 2.7 FDTD simulation of conical lens focusing (*left*, *red*—air, *green*—dielectric) and experimental diffractive conical lens (*right*)

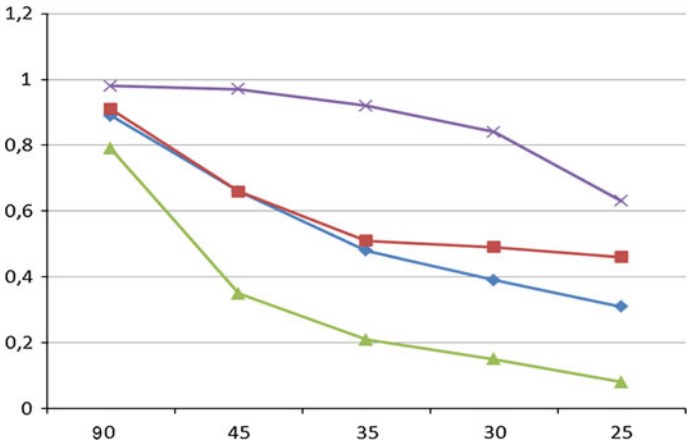

Fig. 2.8 FDTD simulation of resolution power of 3D conical diffractive lenses: *blue*—Δx, *red*—Δy, *green*—Δz, the *purple* curve indicate the asymmetry of focal spot Δx/Δy. The value of Δz is in the unit of classical depth of focus $8\lambda\left(\frac{F}{D}\right)^2$ [1]. All other values are in the unit of Rayleigh radius [1]. At the horizontal axis the cone half-opening angle is shown

The results of simulations in the units of wavelength are shown in the Table 2.1. In approximation the focal spot is ellipse with the length of Δx/λ and Δy/λ in the Table the square of focal spot S are shown. Also the "value" of 3D focal spot V in FWHM on axial direction and lenses Gain are shown in the Table 2.1. The comparison of FDTD simulations and simple approximate algorithm [37] has shown a good agreement. Also it is surprising that simple model of diffractive lens based on several flat metallic annular rings placed along conical surface and normal to optical axis [33, 37] gives the results similar to classical dielectric conical diffractive lens.

Table 2.1 Focusing characteristics of dielectric diffractive conical lenses

α (°)	Δx/λ	Δy/λ	Δz/λ	ΔF/λ	S/λ^2,	V/λ^3	G, dB
90	1.31	1.32	9.2	23	1.36	12.49	11.8
45	0.92	0.91	3.65	13	0.65	2.4	21.1
35	0.67	0.70	2.47		0.37	0.91	21.7
30	0.55	0.68	1.7	6.4	0.29	0.5	21.9
25	0.42	0.67	0.90	2.45	0.22	0.2	22.4

In experimental verification we used a diffractive optical element fabricated on a conical surface. It was manufactured of a numerically controlled lathe, using optical-grade polystyrene with the following optical constants: diffractive index n = 1.59 and absorption coefficient k $\sim 10^{-3}$. The nominal radiation wavelength was λ_0 = 4.6 mm, the lens factor F/D = 1. The initial lens aperture $D/\lambda_0 = 44$ from [7] was limited to a value of $D/\lambda_0 = 20$ by absorption materials to compare with simulations and cone angle α = 35°.

The analysis of the experimental results shows:

- half-width (at half-height) of field intensity distribution along the optical axis for a "conical" diffractive optical element, with parameters as shown above, is twice as narrow as that of an equivalent zone plate (when radiation is incident on the side of the apex of the diffractive optics) and less than $\Delta_z < 2\lambda$;
- when radiation is incident on the side of the base of the diffractive optical element, the width of field intensity distribution along the optical axis is approximately 2.5 times wider than for the equivalent zone plate [7];
- the resolution power of conical lens is about 0.7 of wavelength with full cone angle of 70° in the first case.

It could be noted that the distance from the base of the cone to the focal point $\Delta F/\lambda$ is always $\Delta F > 2\lambda$ (see Table 2.1). Therefore, the longitudinal resolving power (axial resolution) of the diffractive optical element can be controlled by choosing the flexure of the diffractive optical element surface and its spatial orientation and could be less than Abbe barrier. So the "Abbe barrier" was completely broken by such diffractive lenses with unique 3D super resolution.

So in contrast to the flat diffractive optics the curvilinear 3D diffractive conical optics allows for overcoming 3D Abbe barrier with focal distance F more than $F > 2\lambda$. The focal intensity distribution for conical diffractive lens (as for phase reversal flat FZP lens [7, 33]) is also not circularly symmetric and thus the focal spot in the high NA case is no longer an Airy pattern. These results may find useful applications in optical microscopes, including "reverse-microscope", nondestructive testing, microoptics, nanooptics, for manipulate the 3D focused field distribution flexibly by use of diffractive optical elements to some applications and so on.

References

1. Born, M., & Wolf, E. (2005). *Principles of optics*. Oxford: Pergamon.
2. Rigaud, S. J. (ed.). (1841). *Correspondence of scientific men of the seventeenth century* (Vol. 2, pp. 251–255). Oxford: Oxford University Press.
3. Mansfield, S. M., & Kino, G. S. (1990). Solid immersion microscope. *Applied Physics Letters, 57*, 2615–2616.
4. Pimenov, A., Loidl, A. (2003). Focusing of millimeter-wave radiation beyond the Abbe barrier. *Applied Physics Letters, 83*, 4122. doi:10.1063/1.1627474
5. Goldsmith, P. F. (1998). *Quasioptical systems*. New York, IEEE Press
6. Minin, I. V., & Minin, O. V. (2014). Experimental verification 3D subwavelength resolution beyond the diffraction limit with zone plate in millimeter wave. *Microwave and Optical Technology Letters, 56*(10), 2436–2439.
7. Minin, O. V., & Minin, I. V. (2004). *Diffractional optics of millimeter waves*. Boston: IOP Publisher.
8. Minin, I. V., Minin, O. V. (2008). *Basic principles of Fresnel antenna arrays*. Lecture Notes Electrical Engineering (Vol. 19). Berlin, Springer.
9. Minin, I. V., Minin, O. V. (2003). Technology of computational experiment and mathematical modeling of diffractive optical elements of millimeter and submillimeter waveband. In *International Conference "Information Systems and Technologies" IST-2003*, Novosibirsk, NSTU (vol. 1, p. 124–130), April 22–26, 2003.
10. Remcom Incorporated. http://www.remcom.com/html/fdtd.html
11. Yee, K.S. (2010). Numerical solution of initial boundary value problems involving Maxwell's equations in isotropic media. In *IEEE Transaction on AP-14*, 1966, No. 3, pp. 302–307. See also: John B. Schneider. Understanding the Finite-Difference Time-Domain Method 2010. www.eecs.wsu.edu/∼schneidj/ufdtd
12. Minin, I. V., & Minin, O. V. (2013). FDTD analysis of millimeter wave binary photon sieve Fresnel zone plate. *Open Journal of Antennas and Propagation, 1*(3), 44–48.
13. Iwata, S., Kitamura, T. (2011). Three dimensional FDTD analysis of near-field optical disk. In *Progress in Electromagnetics Research Symposium Proceedings* (pp. 157–160). Marrakesh, Morocco, March 20–23, 2001.
14. Minin, I. V., Minin, O. V., Gagnon, N., Petosa, A. (2006). FDTD analysis of a flat diffractive optics with sub-Reyleigh limit resolution in MM/THz waveband. In *Digest of the Joint 31st International Conference on Infrared and Millimeter Waves and 14th International Conference on Terahertz Electronics* (p. 170). Shanghai, China, September 18–22, 2006.
15. Minin, I. V., Minin, O. V., Gagnon, N., Petosa, A. (2007). Investigation of the resolution of phase correcting Fresnel lenses with small focal length-to-diameter ratio and subwavelength focus. In *EMTS*, Canada, Ottawa (URSI), July 26–28, 2007. See also: Minin, I. V., Minin, O. V., Gagnon, N., Petosa, A. Investigation of the resolution of phase correcting Fresnel lenses with small values of F/D and subwavelength focus http://www.computeroptics.smr.ru/KO/PDF/KO30/KO30111.pdf
16. Theory of high numerical aperture focusing. http://www.iitg.ernet.in/physics/fac/brboruah/htmls/hnaf.html
17. Mote, R. G., Yu, R. G., Kumar, A., et al. (2011). Experimental demonstration of near field focusing of a phase micro Fresnel zone plate (FZP) under linearly polarized illumination. *Appl. Phys. B, 102*, 95.
18. Mote, R. G., Yu, S. F., Zhou, W., et al. (2009). Subwavelength focusing behavior of high numerical aperture phase Fresnel zone plates under various polarization states. *Applied Physics Letters, 95*, 191113.
19. Stafeev, S. S., O'Faolain, L., Shanina, M. I., Kotlyar, V. V., Soifer, V. A. (2011). Subwavelength focusing using Fresnel zone plate with focal length of 532 nm. *Computer optics, 35*(4), 460–461 (2011) (in Russian). See also: Kotlyar, V. V., Stafeev, S. S., Liu, Y.,

O'Faolain, L., Kovalev, A. A. (2013). Analysis of the shape of a subwavelength focal spot for the linearly polarized light. *Applied Optics, 52*(3), 330–339.
20. Stafeev, S. S., Kotlyar, V. V. Comparative modeling two methods of sharp focusing with zone plate. *Computer optics, 35*(3), 305–310 (in Russian).
21. Zhang, Y., Zheng, Ch., Zhuang, Y., Ruan, X. (2014). Analysis of near-field subwavelength focusing of hybrid amplitude–phase Fresnel zone plates under radially polarized illumination. *Journal of Optics, 16*, 1-6 015703
22. Minin, I. V., Minin, O. V. (1992). *Diffractive optics* (180 p). NPO InformTEI, Moscow (in Russian).
23. Minin, I. V., Minin O. V. (2011). Reference phase in diffractive lens antennas: a review. *Journal of infrared, millimetre and THz waves, 32*(6), 801–822.
24. Novotny, L., Hecht, B., *Principles of nano-optics.* Cambridge: Cambridge University Press.
25. Minin, I. V., Minin, O. V. (September, 2003) Scanning properties of the diffractive "LENS-PLUS-AXICON" lens in THz, in *Proceedings of the 11th Microcol Symposium*, (pp. 233–236). Budapest, Hungary, September 10–11, 2003.
26. Minin I. V., Minin, O. V. (1989). Optimization of focusing properties of diffraction elements. *Soviet Letters to the Journal of Technical Physics, 15*(23), 29–33.
27. Minin I. V., Minin, O. V. (2004). Scanning properties of diffractive element forming the axial —symmetric diffraction limited wave beam. *Computer optics, 26*, 65–67 (In Russian).
28. Minin, I. V., & Minin, O. V. (2013). Active MMW/terahertz security system based on bessel beams. *ISRN Opticls, 2013*(285127), 1–4.
29. Pacheco-Pena, V., Orazbayev, B., Torres, V., Beruete, M., & Navarro-Cia, M. (2013). Ultra-compact planoconcave zoned metallic lens based on the fishnet metamaterial. *Applied Physics Letters, 103*, 183507.
30. Pacheco-Pena, V., Navarro-Cia, M., Orazbayev, B., Minin, I. V., Minin, O. V., Beruete, M. (2015). Zoned fishnet lens antenna with optimal reference phase for side lobe reduction. *IEEE Transactions on Antennas & Propagation* (accepted).
31. Minin, I. V., Minin, O. V. (2004). Reduction of the zone shadowing effect in diffractive optical elements on curvilinear surfaces. *Optoelectronics, instrumentation and data processing, 40*(3) (2004).
32. Minin, I. V., Minin, O. V. (2004). Correction of dispersion distortion of femtosecond pulses by using the non-planar surface of diffractive optical elements. *Chinese Optics Letters, 08*, 1–4 (2004).
33. Minin, I. V., & Minin, O. V. (2014). 3D diffractive lenses to overcome the 3D Abbe subwavelength diffraction limit. *Chinese Optics Letters, 12*, 060014.
34. Minin, I. V., Minin, O. V. (2004). Correction of dispersion distortion of femtocesond pulses by choosing the surface shape of diffractive optical elements. *Optoelectronics, Instrumentation and Data Processing, 40*(1), 34–38 (2004).
35. Kim, W.-G., Thakur, J. P., & Kim, Y. H. (2010). Efficient DRW antenna for quasi-optics feed in W-band imaging radiometer system. *Microwave and Optical Technical Letters, 52*, 1221.
36. Minin, I. V., Minin O. V. (2014). Spectral properties of 3D diffractive lenses with 3D subwavelengh focusing spot. In *Proceedings of the 12th International Conference on Actual Problems of Electronics Instrument Engineering (APEIE)-34006*(Vol. 1, pp. 485–487). Novosibirsk, October 2–4, 2014.
37. Minin, I. V., & Minin, O. V. (2001). New possibilities of diffractional quasioptics. *Computer optics, 22*, 99. (in Russian).

http://www.springer.com/978-3-319-24251-4

Diffractive Optics and Nanophotonics
Resolution Below the Diffraction Limit
Minin, I.; Minin, O.
2016, XIV, 65 p. 26 illus., 6 illus. in color., Softcover
ISBN: 978-3-319-24251-4